

A Taught-Observe-Ask (TOA) Method for Object Detection with Critical Supervision

Chi-Hao Wu, Qin Huang, Siyang Li, and C.-C. Jay Kuo, *Fellow, IEEE*

Abstract—Being inspired by child’s learning experience - taught first and followed by observation and questioning, we investigate a critically supervised learning methodology for object detection in this work. Specifically, we propose a taught-observe-ask (TOA) method that consists of several novel components such as negative object proposal, critical example mining, and machine-guided question-answer (QA) labeling. To consider labeling time and performance jointly, new evaluation methods are developed to compare the performance of the TOA method, with the fully and weakly supervised learning methods. Extensive experiments are conducted on the PASCAL VOC and the Caltech benchmark datasets. The TOA method provides significantly improved performance of weakly supervision yet demands only about 3-6% of labeling time of full supervision. The effectiveness of each novel component is also analyzed.

Index Terms—Object detection, convolutional neural network, critically supervised learning, active learning, human-in-the-loop, weakly supervised learning, unsupervised learning, pedestrian detection.



1 INTRODUCTION

THE superior performance of convolutional neural networks (CNNs) is attributed to the availability of large-scale datasets with human labeled ground truth. While visual data are easy to acquire, their labeling is time-consuming. There exists a significant gap between labeled and unlabeled data in real world applications. To address this gap, it is essential to develop weakly supervised solutions that exploit a huge amount of unlabeled data and a small amount of carefully selected labeled data to reduce the labeling effort. We address this issue using the object detection task as an example, which is one of the most fundamental problems in computer vision.

Despite extensive studies on weakly supervised object detection in recent years [1], [2], [3], [4], [5], [6], [7], [8], its performance is much lower than that of fully supervised learning. Here, we examine this problem from a brand new angle - how to achieve target performance while keeping the amount of labeled data to the minimum. This is called the “critically supervised” learning methodology since only the most critical data are labeled for the training purpose. This idea is inspired by child’s learning behavior. Children are first taught to recognize objects by parents or teachers given only a few examples. Then, they keep observing the world and start to ask questions. Sometimes, they ask YES/NO-oriented questions to confirm their hypothesis. These questions are from the most critical examples that can enhance their understanding.

It is worthwhile to take a further step to examine the gap between CNN learning and human learning. For CNN-based object detection, large-scale training datasets are needed to train a network with a tremendous number of parameters. To get enough training samples, precise bounding boxes of objects are provided. These fully labeled data are required to generate positive (object) and negative (background) samples simultaneously in training. In human learning, only little supervision is required for positive samples. Besides, humans have innate ability to obtain

background samples either through tracking or 3D vision so that no additional supervision is needed for negative samples.

To reduce the labeling effort for CNNs, we explore the negative object proposal (NOP) concept that collects a huge number of background samples with little supervision. As to positive samples, we argue that it is more natural and faster to apply the question-answer (QA) labeling than drawing tight bounding boxes around objects. According to [9], it takes around 42 seconds to draw a high-quality bounding box while it takes only 1.6 seconds for human to do one QA verification. To reduce the number of questions required to train a high precision detector, a critical example mining (CEM) method is proposed to select the most critical samples through QA. These novel ideas are integrated to yield one new solution called the taught-observe-ask (TOA) method since it mimics how children learn to recognize objects. Being different from the weakly supervised learning methods that get low precision from fewer labels, the TOA method achieves better performance with less labeling time.

The fully supervised training and the critically supervised training methodologies are compared in Fig. 1, where the latter uses the TOA method as an example. Both critical examples and NOP samples are used in the training of a critically supervised TOA method. To be more specific, the CNN model is first trained with a small amount of fully labeled data. Then, extra examples are selected from the set of unlabeled data by using the CEM algorithm. Finally, a series of QAs are conducted for humans to verify labels. Afterwards, the CNN is retrained using critical examples and NOP samples.

There are several major contributions of this work. First, a critically supervised learning methodology is explored to take data labeling and learning into account jointly. Second, the proposed TOA method contains several new ideas such as the negative object proposal (NOP) and critical example mining (CEM) that selects samples for labeling

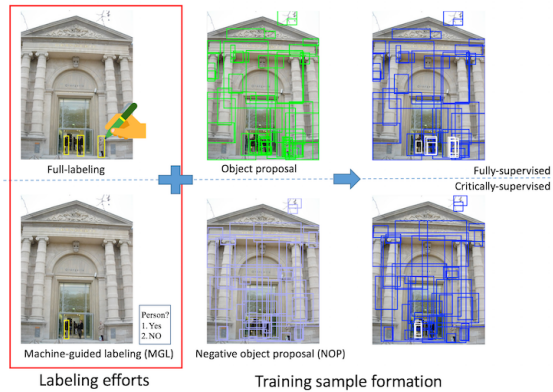


Fig. 1. Comparison of fully-supervised training (top) and critically-supervised training (bottom). All objects are labeled with tight bounding boxes and training samples are obtained from calculating their IoU with object proposals in full supervision. In contrast, critical examples and NOP samples are used in the training of a critically supervised TOA method, where QA labeling is only needed for critical examples selected by the CEM algorithm.

using a dynamically varying rule. Third, new evaluation methods are developed to compare performance against labeling time. Finally, extensive experiments are provided to validate the training strategies and effectiveness of each component in TOA. The TOA method is evaluated on the PASCAL VOC datasets [10] for multi-class object detection, and on the Caltech pedestrian dataset [11] for single-class object detection as a special case. The TOA method provides an mAP (mean Average Precision) improvement of 9.4% over state-of-the-art weakly supervised detectors under the same labeling time. As compared with the fully-supervised learning method, the labeling time saving ranges from 66-95% under the same performance.

2 RELATED PREVIOUS WORK

2.1 Object Detection

Object detection is one of the most intensively studied problems in computer vision. It remains to be a challenging task. Deep learning has brought great success to this area in recent years. Its solution outperforms traditional methods such as the deformable part model (DPM) [12], [13] by a significant margin. The R-CNN [14] accepts each warped region as the CNN input for object classification. Region proposals [15], [16] are needed in the R-CNN. Other CNNs such as the Fast-RCNN [17] and SPP [18] accept the whole image as the input to the CONV layers so as to reduce redundant convolutional computations. Their region proposals are pooled in later layers for further classification and bounding box regression. The Faster-RCNN [19] further extends this idea by including a region proposal network to avoid the need of object proposals outside the network. Recent extensions [20], [21], [22], [23], [24] either provide more efficient implementations with competitive results or keep improving the mAP performance with more advanced network design.

2.2 Weakly Supervised Learning

Weakly supervised object detection is another active research topic since it is not easy to collect a large amount

of labeled data with tight bounding boxes for the training purpose. Given all object classes in one image as the ground truth, weakly supervised object localization (WSOL) techniques are designed to localize the object and enhance the classification accuracy. There has been rapid progress along this line using CNNs [1], [2], [3], [4], [5], [6], [7], [8], [25], [26], [27]. Most of them are based on multiple instance learning (MIL), where images are treated as a bag of instances, and images that contain no object instances of a certain class are labeled as negative samples for this category, and vice versa. However, learning a detector without the bounding box information is challenging. The performance of weakly supervised detectors is significantly lower than that of fully supervised detectors.

2.3 Active Learning and Others

Active learning is a technique that iteratively selects samples from a large set of unlabeled data and asks humans to label so as to retrain more powerful models. Previous active learning work mainly focuses on tasks such as image classification [28], [29], [30], [31] and region labeling [32], [33], [34]. These methods usually start from a good pretrained model and boost its performance with abundant extra unlabeled data. Little work in active learning has been developed for window-based object detection. Another related technique is called "Human-in-the-loop labeling" that considers human-machine collaborative annotation [32], [35], [36]. These methods are used when a pretrained model does not provide satisfying performance on certain challenging tasks and humans are asked to annotate more samples for performance improvement. Several other weakly supervised or unsupervised methods [37], [38], [39] are also related to our work in certain aspects.

3 CRITICALLY SUPERVISED LEARNING

People feed the CNN with a huge amount of labeled data in training, yet some of them are not very critical. For example, fully supervised object detection requires accurate bounding boxes of all target objects in one image, which is time consuming and may not be optimal in striking a balance between efforts and performance. Being inspired by human learning, CNN training can be achieved in a different way. That is, only most relevant samples are labeled. By critically supervised learning, a model is trained to reach a target performance with a minimum amount of labeled samples. This is different from traditional weakly supervised learning, which provides a limited number of labels (or label types) yet does not pay attention to which parts of the dataset are critical to the performance.

Although critically supervised learning is related to active learning or human-in-the-loop labeling as reviewed in Sec. 2.3, it has a clear objective; namely, minimizing the labeling time under a target performance. To achieve the goal, we may adjust labeling strategies dynamically in different labeling stages to ensure that any new labeling effort helps boost the performance. To take object detection as an example, a CNN needs a large number of training samples to gain superior performance while most of them are background (or negative) samples. The acquisition of background

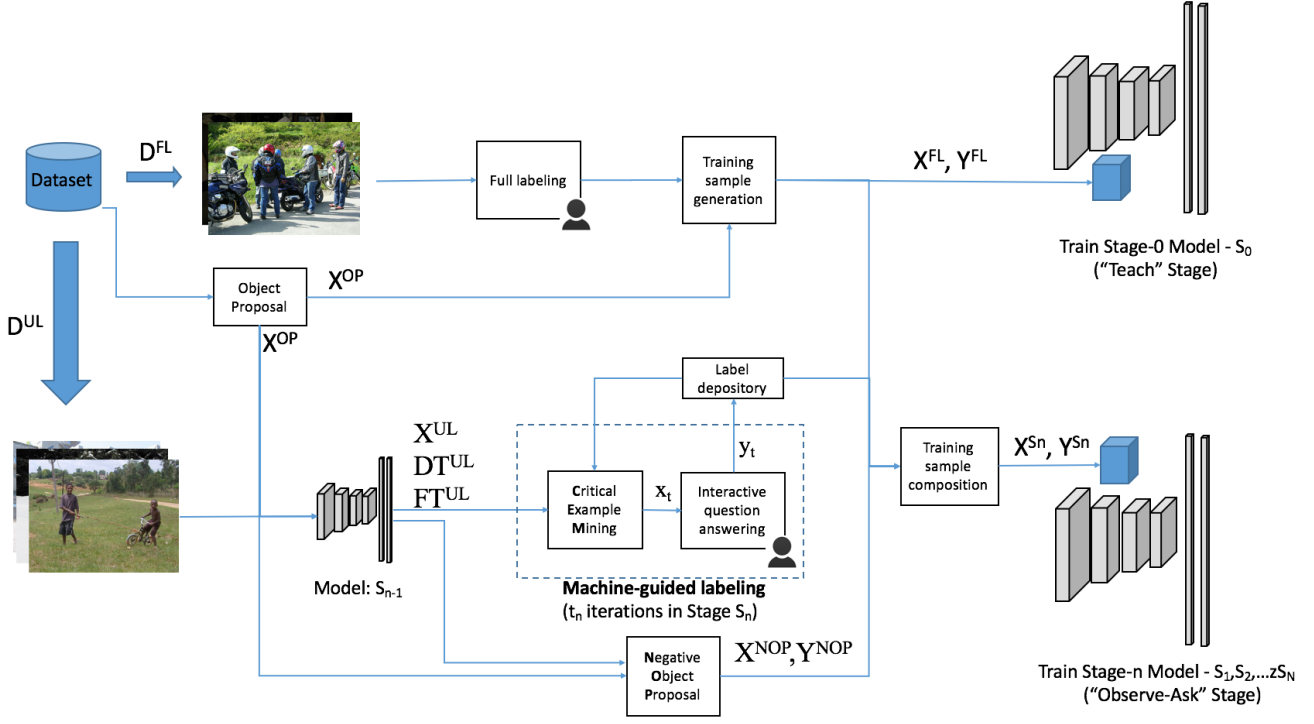


Fig. 2. The system diagram of the proposed TOA method. The upper branch represents the “teach” stage where full labeling is conducted in a small subset of images to train the initial model S_0 . The lower branch is the “observe-ask” stage, where the CEM algorithm is used to select critical examples from an unlabeled dataset using deep features from model S_{n-1} and the QA labeling is conducted on selected examples. The labeled examples are combined with NOP samples to form the training set for stage- n model S_n . Details are given in Sec. 4.

samples relies on accurate labeling of all bounding boxes to avoid false negatives. We will present a new way to provide negative samples more effectively. Furthermore, not all object samples share the same importance. We will show that only a small number of them are representative and critical for a CNN to gain discriminative power in separating different classes. The adoption of various labeling strategies and mining criteria is the key to the success of critically supervised learning.

4 TAUGHT-OBSERVE-ASK (TOA) METHOD

4.1 System Overview

Being inspired by children learning, we propose the TOA method to achieve critically supervised learning. The overall system diagram of the TOA method is shown in Fig. 2. We split a large amount of unlabeled images (D) into two subsets. They are sets of fully labeled and unlabeled images, denoted by D^{FL} and D^{UL} , respectively. Subset D^{FL} consists of only a small number of fully labeled images. Training samples (X^{FL}, Y^{FL}) are generated from them and used to train a stage-0 detector, S_0 , as shown in the upper branch of Fig. 2. This initial stage, called the “teach” stage, is needed for the machine to understand the problem definition, gain basic recognition capability and know what questions to ask in later stages.

All remaining stages are the “observe-ask” stage. In stage n , $n = 1, 2, \dots$, we collect necessary features FT^{UL} and detection scores DT^{UL} for each region proposal using the CNN model trained in the previous stage. The CEM module uses features to mine the most critical example,

x_t , from all unlabeled samples and asks humans to verify (or determine) its label y_t (see Fig. 3). Then, we gather t_n labeled samples through t_n iterations, and combine them with negative object proposals, denoted by X^{NOP} , to form a training set of sample/label pairs (X^{S_n}, Y^{S_n}). A new CNN model, S_n , is then trained using all labeled data up to stage n . We summarized used notations in Table 1. In Fig. 2, the machine-guided labeling (MGL) is used to find the most critical example and conduct question-answer (QA) labeling to obtain labels from humans iteratively. The NOP is used to collect background samples without extra supervision.

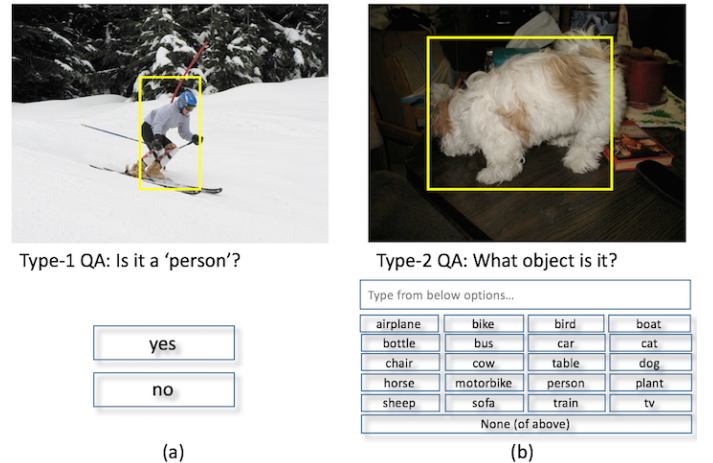


Fig. 3. Illustration of two QA types: (a) type-1 QA and (b) type-2 QA.

TABLE 1

Summary of notations used in this work. Note that N_i^{OP} denotes the number of object proposals in image i and $N^{OP'}$ is different from N^{OP} when only a subset of object proposals are used in the training. $L = \{1 \dots (N + 1)\}$, where $N + 1$ is the total number of object classes and the background is included as an extra class.

Number of images	N^D
Dataset	$D = \{d_i \in Z^{w_i \times y_i} i = 1 \dots N^D\}$
Object proposal	$X^{OP} = \{x_{i,j} \in Z^4 i = 1 \dots N^D, j = 1 \dots N_i^{OP}\}$
	Fully labeled subset
Number of images	N^{FL}
Image index	$\Phi^{FL} = \{\phi_i \in Z i = 1 \dots N^{FL}\}$
Image subset	$D^{FL} = \{d_i \in Z^{w_i \times y_i} i \in \Phi^{FL}\}$
Samples	$X^{FL} = \{x_i \in Z^4 i \in \Phi^{FL}, j = 1 \dots N_i^{OP'}\}$
Labels	$Y^{FL} = \{y_i \in L i \in \Phi^{FL}, j = 1 \dots N_i^{OP'}\}$
	Unlabeled subset
Number of images	N^{UL}
Image index	$\Phi^{UL} = \{\phi_i \in Z i = 1 \dots N^{UL}\}$
Image subset	$D^{UL} = \{d_i \in Z^{w_i \times y_i} i \in \Phi^{UL}\}$
Samples	$X^{UL} = \{x_i \in Z^4 i \in \Phi^{UL}, j = 1 \dots N_i^{OP'}\}$
Labels	$Y^{UL} = \{y_i \in L i \in \Phi^{UL}, j = 1 \dots N_i^{OP'}\}$
Deep Feature	$F^{T^{UL}} = \{f_{t_i} \in R^{dim(ft)} i \in \Phi^{UL}, j = 1 \dots N_i^{OP'}\}$
Detection score	$DT^{UL} = \{dt_i \in R^{N+1} i \in \Phi^{UL}, j = 1 \dots N_i^{OP'}\}$

4.2 Machine-Guided Question-Answer Labeling

Annotating tight bounding boxes (i.e. full labeling) is a time-consuming and demanding job. It is easier to ask humans to answer whether an object class exists in an image yet without the bounding box information (i.e. weak labeling). The drawback of the latter is that its detection performance is lower. In this work, we adopt another labeling scheme, called question-answer (QA) labeling, which can be easily done yet with the bounding box information. We implement two QA labeling types as shown in Fig. 3. For the first one, humans answer the yes-or-no question to verify whether a sample belongs to a certain object class. For the second one, humans choose an object class from a list. They are referred to as type-1 and type-2 QA, respectively. Consecutive type-1 QAs are as effective as a type-2 QA, but the labeling time can be reduced with type-1 QA when we are confident about the object class of the sample.

The TOA method has one more advantage. To make training effective, humans need to label all objects in one image without missing any objects in fully or weakly supervised schemes. Failing to do so will result in performance drop. Thus, extra efforts are required for verification. The need to label all objects is eased by the adoption of NOP in the TOA method. In other words, annotators only need to focus on one specific sample at a time.

It is, however, not always possible for the machine to select samples with perfectly tight bounding boxes for QA. In the QA-labeling process, we require humans to give answers with tolerance to noisy samples (i.e. samples without perfect bounding boxes). A guideline is provided to annotators. For example, they should accept objects when the sample overlaps with the drawn bounding box with the intersection-over-union (IOU) over a certain threshold value (e.g., 0.6). A few examples that meet the threshold values are provided to annotators in the beginning of the annotation process. Humans can learn such a rule quickly. Although small variations may still occur when the overlapping degree is close to 0.6, the final performance is not

much affected as shown in Sec. 6.

4.3 Negative Object Proposal (NOP)

The object proposal [15], [16] is a technique to extract a set of bounding boxes that ideally include all objects in one image. It reduces the computational complexity of exhaustive search. Here, we present a scheme, called the negative object proposal (NOP), that collects a set of boxes that contain no objects. With the NOP, the need of labeling all objects in one image to collect negative samples is eliminated.

Distinguishing objects from non-objects appears to be effortless for humans, yet unsupervised NOP extraction is not a trivial job. To show the challenge, we examine two ways to extract the NOP. First, we collect boxes with extremely low scores from an object proposal algorithm called the EdgeBoxes [15]. Second, we modify the formula of EdgeBoxes to weigh more on boxes that have more edges going across box boundaries. The results are shown in Fig. 4. We see two major problems in these results. First, the algorithms tend to contain many small bounding boxes. To train a CNN, the NOP should contain some informative samples of reasonable sizes and overlap with objects to a certain degree. Second, reasonable training performance could only be achieved with high NOP accuracy since negative samples are the majority in the training samples. However, the boxes generated by these algorithms occasionally contain positive samples and fail to meet the required precision.

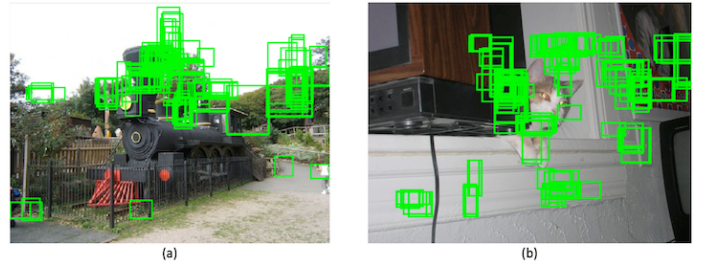


Fig. 4. Examples to illustrate the challenges in extracting good NOP samples, where only 200 out of all boxes are plotted for ease of visualization: (a) edge-box results with extremely low scores which rank over 2000 in one image and (b) the edge-box results with the modified formula.

To address these challenges, we use the detection score information DT^{UL} from the stage-0 detector only. In other words, we do not need extra labeling efforts for the NOP. Although the stage-0 model is trained by a small percentage of data and its detection scores are not robust, one can still obtain a candidate set of samples that contain almost all objects with a sufficiently low threshold. Then, NOP samples can be extracted by avoiding samples that are spatially close to the candidate set. This idea can be formalized mathematically below.

We first define an inverse set concept based on the IoU, where the function returns samples in set A that do not have a large overlap degree with any samples in set B:

$$C = \text{InvSet}(A, B) = \{a_i \in A | \text{IoU}(a_i, b_j) < \tau, \forall b_j \in B\}. \quad (1)$$

With Eq. (2), the NOP set can be calculated by finding the inverse set from a candidate object set that is extracted using detection scores. It can be written as

$$X_i^{NOP} = \text{InvSet}(X_i^{OP}, X_i^{DT_\epsilon}), \quad \forall i \in \Phi^{UL}, \quad (2)$$

where X^{DT_ϵ} is the candidate set fetched by applying threshold ϵ to detection scores and X^{OP} contains samples generated by an object proposal algorithm. The resulting NOP set, X^{NOP} , not only provides high quality negative samples of reasonable sizes but also has a very low probability to include object samples. Experiments will be conducted in Sec. 6.5 to support such a claim.

It is sometimes possible to create the NOP samples without any supervision (e.g. without the stage-0 detector) if we have prior knowledge about target objects. For example, for the pedestrian detection problem, almost all pedestrians are in the upright direction with a certain range of aspect ratios. We can simply make the candidate object set contain boxes whose shapes are in the range of all possible pedestrian aspect ratios. The NOP calculated from Eq. (2) will generate boxes of wrong pedestrian aspect ratios. This is used in experiments in Sec. 6, and we obtain good performance even if it is totally unsupervised.

4.4 Critical Example Mining (CEM)

It is well known that some samples play more important roles than others in the CNN training as elaborated in [40], [41]. Typically, hard samples are more critical to performance improvement. In critically supervised learning, we claim that the criteria of choosing important samples should change dynamically along the labeling process, and use Fig. 5 to support this claim. For a limited labeling budget, the selection of examples should be cautious so as not to waste any labeling effort. Initially, two criteria are more important: 1) the selection should be balanced across different classes; and 2) the sample should be representative, and redundant ones should be avoided. As shown in the top row of Fig. 5, cautious selection of labeled samples using these two criteria is adequate. As more samples are labeled and the model starts to gain good performance on easy samples, it becomes important to find harder examples to achieve better separation in decision boundaries as shown in the bottom row of Fig. 5. This type of CEM is a new problem that has never been addressed before, to the best of our knowledge.

We define a function, $c_{i,j}$, to capture the criticalness of each sample by taking three components into consideration. They are class balancing (BAL), sample representativeness (REP), and hardness (HARD). The criticalness function can be written as the sum of these three components:

$$c_{i,j} = c_{i,j}^{BAL} + c_{i,j}^{REP} + c_{i,j}^{HARD}, \quad (3)$$

where

$$c_{i,j}^{BAL} = cs_{i,j}^{BAL} \cdot cp_{i,j}^{BAL}(t), \quad (4)$$

$$c_{i,j}^{REP} = cs_{i,j}^{REP} \cdot cp_{i,j}^{REP}(t), \quad (5)$$

$$c_{i,j}^{HARD} = cs_{i,j}^{HARD} \cdot cp_{i,j}^{HARD}(t). \quad (6)$$

Since the importance of each component varies along the labeling process, we express it as the product of two terms. The first term, $cs_{i,j}$, represents its score function while the

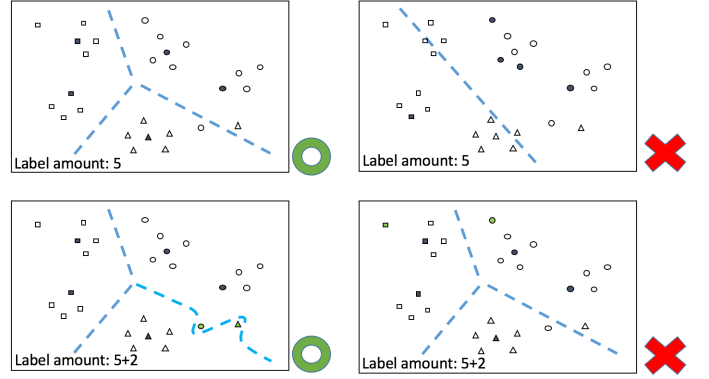


Fig. 5. Illustration of the critically-supervised learning methodology, where solid samples are labeled samples while other are unlabeled ones. Top) Under the constraint of using only 5 QAs, selection of samples for labeling has major impact on the trained detector (classifier). The left choice is good while the right choice is poor. Bottom) When additional 2 samples (in green) can be selected to achieve better performance, the selection rule is changed. Again, the left choice is good while the right choice is poor.

second term, $cp_{i,j}$, called the progress function, controls the varying contribution of each component in the t th iteration. There is no ground truth about importance of each sample along the labeling process, and this function is chosen heuristically. Before explaining each component, we examine the characteristics of the criticalness function.

Detection Score and Deep Features. The detection score, $dt_{i,j}$, is the output of the CNN that represents the probability of a sample belonging to a specific class. They are obtained in each stage- n by feeding all training samples into the S_{n-1} model for prediction. Although the precision of S_{n-1} may not be high enough, its detection score of a sample still serves as an indicator of how likely the sample could be an object. Each score $dt_{i,j}$ is a vector with a dimension of $(N + 1)$ (i.e., N object classes plus one background class). Besides detection scores, deep features can be extracted from CNN prediction and they provide useful information in mining critical examples. Deep features, FT , are the output from one of the intermediate CNN layers and the feature dimension depends on which layer in use. Detailed experimental set-ups will be provided in Sec. 6.

KNN Graph and Geodesic Distance. To measure the representativeness of a sample, we design our mining algorithm based on the k-nearest-neighbor (kNN) graph. To build the undirected kNN graph $G = (V, E)$, each node is a sample in either X^{UL} or X^{FL} . We calculate the Euclidean distances of each node v_i with other samples in the deep feature space, which is denoted by $d(v_i, V)$. Sample v_2 is set to connect with v_1 in the graph if it is among the k nearest neighbors of v_1 . One can draw the kNN graph based on the following formula:

$$e_{v_1, v_2} = \begin{cases} 1, & d(v_1, v_2) \leq \text{ascend-sort}(d(v_1, V))[K], \\ 1, & d(v_1, v_2) \leq \text{ascend-sort}(d(v_2, V))[K], \\ 0, & \text{otherwise.} \end{cases} \quad (7)$$

With the kNN graph, the geodesic distance between two nodes is the shortest path between two nodes in the kNN graph [38]. As compared with the Euclidean distance, the geodesic distance better represents the sample distribution

over the deep feature space. For each unlabeled sample, we define a metric, $ldist_{i,j}$, to represent the nearest labeled sample measured by the geodesic distance. When $ldist_{i,j}$ is smaller, sample $x_{i,j}$ is less critical since there is a labeled sample nearby. An exemplary kNN graph and its associated geodesic distance and DLIST metric are shown in Fig. 6.

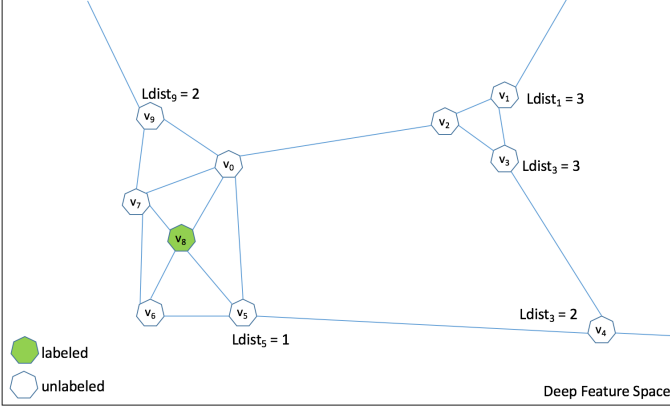


Fig. 6. Illustration of the kNN graph where each node is connected to its K nearest neighbors ($K=3$ in this example). The $Ldist$ of a node is the number of edges along the shortest path to its nearest labeled node.

Progress Function. To control the contribution of each component in the criticalness function dynamically, we define a simple progress function below:

$$P(x, \mu, \sigma^2) = \begin{cases} 1, & x < \mu, \\ N(x|\mu, \sigma^2)/N(\mu|\mu, \sigma^2), & x \geq \mu, \end{cases} \quad (8)$$

where $N(x|\mu, \sigma^2)$ is the Gaussian with mean μ and variance σ^2 . A component is set to be important in the labeling process until a certain condition is met at threshold μ . After that, we reduce its weight gradually in Gaussian decay form. Then, we can move the focus to other criteria in critical examples selection.

Criticalness Function. We elaborate on the three components of the criticalness function. The sample balancing (BAL) component considers the balance between different object classes and the balance between positive and negative samples simultaneously. In earlier labeling stages, there are much more negative samples obtained by the NOP algorithm. Selecting a sample with a higher probability of positive samples is important so that the QA effort is not wasted. Hence, the maximum detection score, $\max(dt_{i,j})$, of a sample serves as a good index in sample selection; namely,

$$c_{i,j}^{BAL} = \max(dt_{i,j}) \cdot P(\text{count}(y_{i,j} > 0, \forall y_{i,j} \in Y_i^{UL}), (\mu, \sigma^2)^{BAL1}) \cdot P(\text{count}(y_{i,j} = \text{argmax}(dt_{i,j}), \forall y_{i,j} \in Y^{UL}), (\mu, \sigma^2)^{BAL2}).$$

This contains two progress functions. The first one is to lower BAL's importance when more object samples are labeled. The second one is to ensure the balance between different classes. This is achieved by setting a threshold at which a specific class already has enough labeled samples in the current stage. For instance, we can avoid selecting too many examples from major classes such as "people" or "car" in the VOC dataset and give the QA quota to other rare classes to boost the overall performance in earlier stages.

The sample representativeness (REP) component considers the representativeness of a sample. As discussed earlier,

when $dlist_{i,j}$ is smaller, the sample is relatively redundant in training, and vice versa. Thus, we have

$$c_{i,j}^{REP} = \delta \cdot -P(ldist_{i,j}, (\mu, \sigma^2)^{REP}). \quad (9)$$

where $DLIST$ is in the progress function since its values may keep changing in the labeling process. Besides the progress function, we use variable δ to adjust the importance of this component across different datasets. Some datasets contain much more redundant samples while others not. The choice of δ is determined by the sample distribution in the kNN graph and will be further discussed in Sec. 6.5.

The hardness (HARD) component gives a higher priority to hard samples which appear in decision boundaries. This component is not critical until many representative samples are labeled. We define

$$c_{i,j}^{HARD} = \left(\sum (dt_{i,j}) - \max(dt_{i,j}) \right) \cdot -P(\text{mean}(DLIST), (\mu, \sigma^2)^{HARD}), \quad (10)$$

where the progress function is determined by the average $DLIST$ value since it is an indicator of how densely samples are labeled in the deep feature space. This component is important only when labeled samples are dense enough in the feature space. To determine the hardness of a sample, we examine the detection scores and check if they are high not only in one but in several object classes.

The criticalness score is used to determine the importance of a sample. The CEM procedure computes the criticalness scores of all unlabeled samples, and the sample with the highest score is selected for the QA labeling. In general, we apply the type-1 QA labeling by asking humans whether the sample belongs to the class that has the highest score. For hard samples which satisfies $cp_{i,j}^{HARD} > cp_{i,j}^{BAL}$ and $cp_{i,j}^{HARD} > cp_{i,j}^{REP}$, the type-2 QA is used since we are less sure about its class. The newly labeled sample is used to update $dlist_{i,j}$ and $c_{i,j}$ values of affected unlabeled samples. The iteration continues until the end of the stage.

4.5 Training Sample Composition

In TOA, we obtain some QA-labeled samples and NOP samples from unlabeled images in each stage. To train the model, positive samples are chosen among object proposals that have IoU greater than a threshold TH_{FG} with QA-labeled positive samples. Negative samples are selected from the NOP set with its IoU in the range of $[TH_{HI}, TH_{LO}]$ with QA-labeled positive samples. The three thresholds are similar to that used in fully supervised learning. The differences lie in that we use QA-labeled samples to calculate the IoU value and determine positive/negative samples rather than the ground truth and that we use the NOP instead of object proposals for negative samples. Examples will be shown in Sec. 6.5. After the QA number reaches the target amount in stage n , the newly labeled images associated with the QA-labeled samples as well as all previous labeled data are used to train CNN model S_n .

It is worthwhile to point out that QA-labeled samples can be noisy (i.e. the bounding boxes may not be tight). The composition of samples in the TOA method with three thresholds may cause positive samples to have less overlapping with the real ground truth and/or negative samples to

have more overlapping with the ground truth than the fully supervised case. We will elaborate on the corresponding IoU distributions in Sec. 6.5.

5 EVALUATION METHOD

5.1 Labeling Time Model

Human labeling time has been discussed in prior literature. For example, it was mentioned in [9] that drawing a tight bounding box with high quality takes around 42 seconds in crowd sourcing, and 26 seconds for faster annotation. In contrast, the labeling time for a simple yes-or-no question only requires 1.6 seconds. Similar numbers were reported in [42], [43].

In order to evaluate the performance, we need to build a labeling time model. Here, we use the numbers mentioned in these papers for bounding box drawing and yes-or-no questions. In addition, we need the labeling time for answering a type-2 question (*i.e.*, what class an object belongs to). We conduct experiments on our own, and calculate the average time needed to type a specific object class in multiple trials. It is 2.4 seconds. Similarly, we evaluate the time for humans to scan the whole image to ensure no missing objects, which is 2.6 seconds. These four numbers are summarized in Table 2 under the column of the high-quality (HQ) profile. We also provide the moderate-quality (MQ) profile in Table 2. The MQ profile allows quicker drawing of bounding boxes and assumes that image verification is done in parallel while drawing boxes. Experimental results in Sec. 6.5 demonstrate that the proposed TOA method is competitive in both profiles.

In this table, we also use a variable to denote a specific labeling time to accommodate different labeling models since powerful tools can be designed for more efficient annotation. For example, we can show a bunch of samples together and make humans click on those that do not belong to a certain class. This batch process will make the yes-or-no question faster than 1.6 seconds per image in average.

TABLE 2

The labeling time model with different labeling types, where the HQ profile is used for high-quality labeling and the MQ profile is for moderate quality labeling.

Labeling type	variable	HQ profile	MQ profile
Draw a tight bounding box	t^{FL}	42.0 sec	26.0 sec
Answer type-1 question	t^{QA1}	1.6 sec	1.6 sec
Answer type-2 question	t^{QA2}	2.4 sec	2.4 sec
Verify missing objects	t^{VER}	2.6 sec	0.0 sec

5.2 Estimated Labeling Time Ratio (ELTR)

Given the labeling time model, we define a quantity, called the estimated labeling time ratio (ELTR), to measure the overall performance as compared to the fully or weakly supervised schemes. The ELTR calculates the labeling time needed for a specific method normalized by the time required for fully labeling for the whole image set. We provide detailed calculation of ELTR for different training scenarios below.

If we use a subset of images, D^{FL} , in fully supervised training, its ELTR is the ratio between the number of selected image and the whole dataset:

$$ELTR^{FS} = N^{FL}/N^D. \quad (11)$$

For weak supervision, humans need to answer object classes in one image. This is the same as the type-2 question answer. The difference is that humans have to answer all object classes in one image in weak supervision. Suppose that there are N_i^{CLS} classes in image i , it takes N_i^{CLS} times t^{QA2} seconds for weak supervision for this image. Moreover, verification on the whole image has to be done in weakly supervised learning. Thus, we have

$$ELTR^{WS} = \frac{\sum_{i=1}^{N^D} (t^{VER} + t^{QA2} N_i^{CLS})}{\sum_{i=1}^{N^D} t^{FL} \cdot N_i^{OBJ}}, \quad (12)$$

where N_i^{OBJ} denotes the number of object presented in image i . The labeling time is normalized by the time needed for full labeling of the whole dataset. For critical supervision, our TOA method includes full-labeling, and type-1 and type-2 QA labeling. All of them are added up to yield

$$ELTR^{CS} = \frac{\sum_{i \in \Phi^{FL}} t^{FL} N_i^{OBJ} + t^{QA1} N^{QA1} + t^{QA2} N^{QA2}}{\sum_{i=1}^{N^D} t^{FL} N_i^{OBJ}}. \quad (13)$$

where N^{QA} is the total QA number and N^{QA1} and N^{QA2} are the total QA numbers for type-1 and type-2 questions, respectively.

6 EXPERIMENTAL RESULTS

6.1 Datasets

To validate the proposed TOA method, we first test our algorithm on the general multi-class object detection problem using the VOC 2007 and the VOC 2012 dataset (abbreviated as VOC07 and VOC12, respectively). To further demonstrate the generalization capability of the TOA method, we conduct experiments on the Caltech pedestrian dataset (abbreviated as the Caltech dataset), which is a special case of object detection with only one object class.

VOC Dataset. The VOC07 and the VOC12 datasets are two most widely used object detection datasets. They provide 20 commonly seen object classes. The VOC datasets are split into three subsets - train, val, and test sets. In our work, we follow the standard procedure to train our model on the trainval set and calculate the mean average precision (mAP) on the test set. The VOC07 dataset has a total of 5011 trainval images while the VOC07+12 dataset has a total of 16553 trainval images.

Caltech Dataset. The Caltech dataset is the mostly used pedestrian detection dataset. It provides a large number of training images captured from the street with wide diversity. Pedestrian detection is essential to various applications such as autonomous vehicles, the advanced driving assistant system (ADAS), security, robotics, and others. It is a special case of object detection which focuses on one object class only. However, it has several challenges such as cluttered background, occlusion, extremely small objects, etc. The Caltech dataset provides a total of 128419 training images with their bounding box ground truth.

6.2 Experimental Setup

Simulation. The TOA method involves iterative human-machine collaborative labeling. To provide fair comparison with fully supervised and weakly supervised learning methods, we choose to use existing datasets that are already annotated. However, we do not use their labels directly. Instead, we simulate our results by applying the QA-labeling and let the ground truth in the dataset to answer our questions. For example, when we choose a sample and ask a type-1 question, we assume that humans will give the answer “yes” when the sample has high enough IoU with the ground truth, and the class that we query fits what is annotated in the ground truth. For type-2 questions, we are expected to get the object classes when IoU with the ground truth is greater than a threshold. By doing the simulation, no human labeling is really needed. In our work, the IoU threshold is set to 0.6. We will provide more analysis on the variation of the IoU threshold in Sec. 6.5.

Network Architecture. The evolution of CNN architecture is very fast nowadays, and so is the CNN performance improvement on different problems. In this work, we adopt the Fast-RCNN [17] (abbreviated as the FRCNN) as the baseline method for the proof of concept. The FRCNN does not provide state-of-the-art object detection performance. We adopt it for two reasons. First, weakly supervised object detection methods are still mostly based on FRCNN so that we use it for fair comparison. Second, the FRCNN is a well-known method in computer vision. Considering that few CNNs have been tested on both the Caltech and the VOC datasets, the FRCNN is a good choice [17], [44]. Here, we use the VGG-16 [45] as the back-bone network pretrained by the ImageNet dataset.

Implementation Details. In stage-0, a subset of images is selected for full supervision. This subset is randomly selected from the whole training set in the setup. Note that we tried different random sets and the results do not change much. For object proposals, we adopt the Edgeboxes [15] algorithm with its default settings. In the OA-stage, we select the responses at the FC-7 layer of the CNN as the deep features denoted by FT . The FC-7 is the last layer of the VGG-16 network. Its feature space contains multiple clusters that fit the TOA method well.

To determine detection scores and deep features for unlabeled training images, the non-maxima-suppression (NMS) technique is adopted to reduce redundant samples. In generating the kNN graph, each sample is computed its Euclidean distance with all other samples, and the computational overhead is high. To accelerate the process, we exclude samples with detections scores lower than 0.01. According to the designed CEM, these samples are almost impossible to be selected. Furthermore, we generate the kNN graph using the CUDA to exploit the GPU parallelism, which is about 200 times faster than the CPU implementation. We set $K = 4$ for the kNN graph.

Other parameters are empirically set as $\tau = 0.3$, $\epsilon = 0.01$, $(\mu, \sigma^2)^{BAL1} = (1, 0.2)$, $(\mu, \sigma^2)^{BAL2} = (\#QA/20, 1)$, $(\mu, \sigma^2)^{REP} = (1.5, 0.5)$, and $(\mu, \sigma^2)^{HARD} = (2, 0.2)$, $(TH_{FG}, TH_{HI}, TH_{LO}) = (0.6, 0.4, 0.1)$. Other training options (e.g. REG, PRETR, WTR) will be discussed later in Sec. 6.6.

6.3 Multi-Class Object Detection

We validate the TOA method on the VOC07 dataset in this subsection. To compare critical, full and weak supervision methods, we show a mAP-vs-ELTR plot in Fig. 7, where the HQ profile is used for ELTR calculation. In the figure, the points on the blue curve are trained using full supervision with different sizes of image subsets. The black point of triangle shape on the curve is the state-of-the-art weak supervision performance. Under the same mAP, its labeling time is less than that of full supervision. The points on the red curve show the performance of the TOA method in different stages. The TOA method has a higher mAP than the weak supervision method. It also demands much less labeling time than full and weak supervision methods.

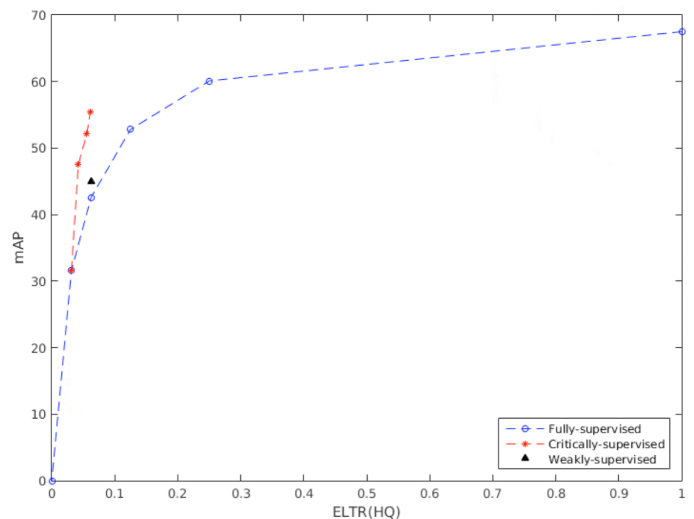


Fig. 7. The MAP-vs-ELTR performance comparison of fully, weakly, and critically supervised learning on the VOC07 dataset, where each dot denotes a model trained using different training sets with the estimated labeling time.

In this experiment, our S_0 model uses only 157 images, which are 1/64 of the VOC07 trainval set. Then, different QA numbers are conducted in each stage, as detailed in Table 3. For example, in stage-1, 3600 QAs are done and the mAP of S_1 boosts from 32.0% to 47.5% with only 0.0421 ELTR required. In stage-2, an additional 3600 QAs are performed. A total of 7200 QAs contribute to a mAP of 52.2% with 0.0559 ELTR. In stage-2, some QAs are of type-2 which are decided by the CEM algorithm.

TABLE 3

The experimental setup for Fig. 7, where the numbers in parenthesis after FRCNN means the percentage of data used for labeling. The parenthesis after TOA means the number of stages used in TOA. In this table, the numbers of full-labeled images and QA-labeled samples are provided along with the final estimated labeling time ratio (ELTR).

method	Category	mAP	N^{Full}	N^{QA1}	N^{QA2}	N^{QA}	ELTR(HQ)
FRCNN	Full supervision	67.5	5011	0	0	0	1
FRCNN(1/4)	Full supervision	60.1	1253	0	0	0	0.25
FRCNN(1/8)	Full supervision	52.8	626	0	0	0	0.125
FRCNN(1/16)	Full supervision	42.6	313	0	0	0	0.0625
FRCNN(1/32)	Full supervision	32.0	157	0	0	0	0.0313
K-EM [1]	Weak supervision	46.1	0	0	0	0	0.0619
TOA(S1)	Critical supervision	47.5	157	3600	0	3600	0.0421
TOA(S2)	Critical supervision	52.2	157	5276	1924	7200	0.0559
TOA(S3)	Critical supervision	55.5	157	5276	3124	8400	0.0613

The benefits of the TOA method can be examined from two aspects. For the same labeling time with ELTR equal to 0.062, the TOA can achieve a 55.5% mAP, which outperforms K-EM (weakly supervised method) by 9.4%, and exceeds FRCNN by 12.9%. On the other hand, under the same mAP of 55%, the labeling time needed for the TOA method is only about one third of the labeling time of the FRCNN while weak supervision cannot reach this level. The detection performance on different classes is shown in Table 4. The TOA method can achieve consistent improvement across all object classes.

Besides the VOC07 dataset, we apply the TOA method to the VOC07+12 trainval dataset, and test it on the VOC07 test set. Since the number of images becomes larger, the setup of the TOA method is different and it is given in Table 5. Similar performance gains can be observed, and a higher mAP of 58.3% is achieved with an even lower ELTR.

6.4 Single-Class Object Detection

In this subsection, we evaluate the TOA method on the single object detection problem using the Caltech dataset. The standard evaluation metric for the Caltech dataset is the miss rate (MR) versus the false-positive-per-image (FPPI) curve, which is calculated for each trained model. Then, the overall performance of a model is obtained by averaging several reference points on the curve in log scale. We use the MR to represent the log-average-miss-rate, and compare the performance of the TOA method with the full supervision scheme in Fig. 8. In these experiments, we implement the FRCNN adapted to the pedestrian detection problem according to [44]. We see from the figure that the performance gain is even more obvious for the Caltech dataset. For example, when $MR = 17$, the TOA can save up to 95% of the labeling efforts as compared to that of the full supervision method. This is attributed to fact that the Caltech dataset contains more redundant samples than the VOC datasets. The Caltech dataset is captured frame-by-frame with street-view scenes, and most pedestrians have similar shapes and appearances. Clearly, the TOA method has an advantage when a dataset has more similar (or redundant) samples.

The detailed setup of our experiment is given in Table 6, where each entry gives a dot on the the MR-vs-ELTR curve. The MR-vs-FPPI (false-positive-per-image) curves of these models are shown in Fig. 9. Although the Caltech dataset provides frame-to-frame images, we use one image every 4 frames to form our baseline dataset D . This is because that the computational time can be saved dramatically during the whole TOA process, and the performance with one quarter of training data is not much different from that of using every frame as shown in Table 6.

6.5 Analysis on CEM, NOP and Labeling Time Models

We conduct further analysis on CEM, NOP and labeling time models on the VOC07 dataset to gain more insights into the TOA method.

Effectiveness of CEM. We attempt to explain the proposed CEM algorithm. First, we justify the use of detection scores in the criticalness function. The valid QA rates are provided in Table 7, which indicate the QA percentages that result in labeled objects but background. As mentioned before,

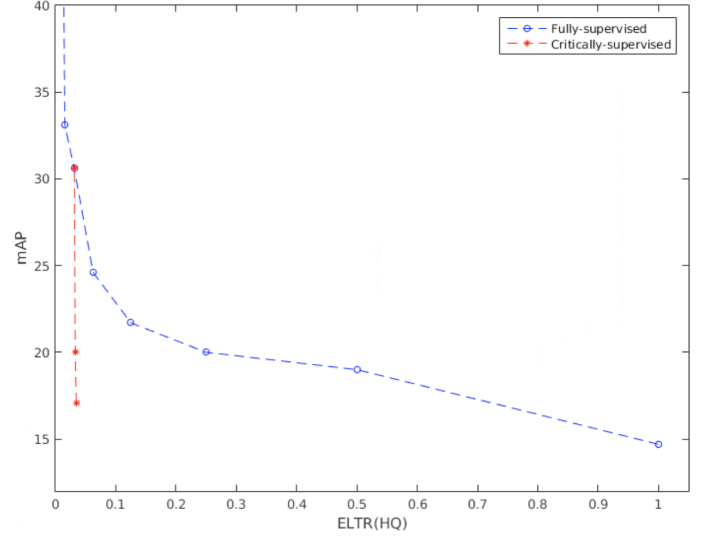


Fig. 8. The MR-vs-ELTR performance comparison of fully and critically supervised learning on the Caltech dataset, where each dot denotes a model trained under different setups with their associated labeling time.

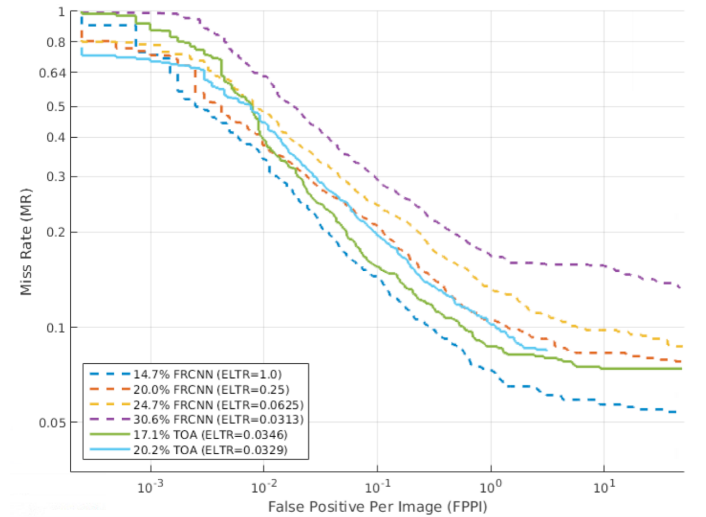


Fig. 9. The MR-vs-FPPI performance curves for models defined in Table 6.

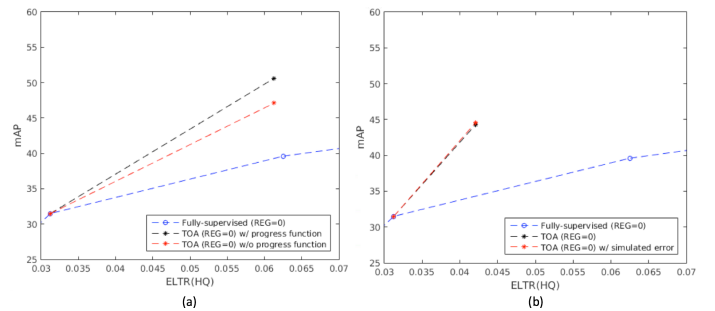


Fig. 10. Analysis results for the TOA method: (a) the effectiveness of the progress function for hard samples, and (b) the results by taking human errors into account in the simulation.

only object samples can help improve the precision since we already have NOP samples. For the type-1 QA to be a valid one, the sample has to be an object and the class

TABLE 4
Comparison of detection results for each object class with the experimental setup given in Table 3, and visualized in Fig. 7

method	aero	bike	bird	boat	bottle	bus	car	cat	chair	cow	table	dog	horse	mbike	person	plant	sheep	sofa	train	tv	mAP
FRCNN(1/32)	24.8	27.4	30.2	11.7	14.8	34.4	56.9	44.4	18.3	43.8	17.7	37.7	52.4	45.3	51.2	11.2	32.0	24.9	23.4	36.7	32.0
FRCNN(1/16)	39.9	58.2	42.6	28.0	15.8	50.3	66.4	59.1	29.2	46.4	30.4	44.8	54.3	62.6	54.5	14.3	24.0	32.9	43.9	53.9	42.6
FRCNN(1/8)	47.4	65.4	50.0	34.4	24.9	65.6	71.7	69.0	28.3	62.9	41.2	64.3	70.2	62.6	61.8	23.3	59.6	51.8	53.1	49.1	52.8
FRCNN(1/4)	58.8	70.4	58.1	42.9	43.6	70.7	75.9	76.2	34.4	66.3	52.4	69.5	76.4	73.6	67.5	32.6	59.3	56.6	63.7	52.6	60.1
FRCNN	68.6	77.8	65.0	57.5	44.8	79.9	78.6	83.8	41.6	74.5	62.0	82.3	80.8	75.3	70.8	37.7	66.2	68.0	75.4	60.0	67.5
K-EM	59.8	64.6	47.8	28.8	21.4	67.7	70.3	61.2	17.2	51.5	34.0	42.3	48.8	65.9	9.3	21.1	53.6	51.4	54.7	50.7	46.1
TOA(S1)	48.1	61.5	43.6	22.5	29.6	60.8	61.7	56.1	24.8	57.3	28.4	56.4	63.7	62.9	47.7	21.5	47.8	45.6	55.9	54.5	47.5
TOA(S2)	53.6	48.3	55.3	31.0	27.2	61.1	66.9	70.2	26.1	68.8	32.3	66.8	71.1	62.8	57.2	21.8	54.0	52.0	64.5	52.1	52.2
TOA(S3)	60.0	52.8	57.6	35.3	29.6	66.3	69.2	73.2	29.5	70.3	42.5	66.5	72.8	66.2	58.4	26.2	57.5	54.3	65.4	57.2	55.5

TABLE 5

The experimental setup for the fully and critically supervised CNNs trained on the VOC07+12 trainval dataset and tested on the VOC07 dataset. The numbers of full-labeled images and QA-labeled samples are provided along with the final estimated labeling time ratio (ELTR).

method	Category	mAP	N^{Full}	N^{QA1}	N^{QA2}	N^{QA}	ELTR(HQ)
FRCNN	Full supervision	70.7	16551	0	0	0	1
FRCNN(1/4)	Full supervision	66.8	4138	0	0	0	0.25
FRCNN(1/8)	Full supervision	61.6	2069	0	0	0	0.125
FRCNN(1/16)	Full supervision	56.1	1034	0	0	0	0.0625
FRCNN(1/32)	Full supervision	49.0	517	0	0	0	0.0313
FRCNN(1/64)	Full supervision	38.3	259	0	0	0	0.0156
TOA(S1)	Critical supervision	54.6	259	10000	0	10000	0.0248
TOA(S2)	Critical supervision	58.3	259	16038	3962	20000	0.0357

TABLE 6

The experimental setup for Fig. 8, where the TOA method is applied to a subset(1/4) of the Caltech dataset so that the ELTR for FRCNN(1/4) is equal to one.

	MR	N^{Full}	N^{QA1}	N^{QA2}	N^{QA}	ELTR(HQ)
FRCNN	14.4	128419	0	0	0	
FRCNN(1/4)	14.7	32105	0	0	0	1
FRCNN(1/8)	19.0	16052	0	0	0	0.5
FRCNN(1/16)	20.0	8026	0	0	0	0.25
FRCNN(1/32)	21.7	4013	0	0	0	0.125
FRCNN(1/64)	24.6	2007	0	0	0	0.0625
FRCNN(1/128)	30.6	1003	0	0	0	0.0313
TOA(S1)	20.2	1003	50000	0	5000	0.0329
TOA(S2)	17.1	1003	10000	0	10000	0.0346

should be correct. For the type-2 QA to be a valid one, it requires the sample to be an object only. Since the initial model S_0 is a weak detector, the valid QA-1 rate is only around 37% in stage-1. Thus, it is important to use samples of high detection score for the QA in early stages. Otherwise, more QAs will be wasted.

TABLE 7

The valid QA rate with the CEM algorithm in each stage.

	QA1	Valid QA1	QA2	Valid QA2
TOA(S1)	3600	1320	0	0
TOA(S2)	5276	1754	1924	904
TOA(S3)	5276	1754	3124	1406

Second, we justify the class balancing component in the progress function. We compare the original detection result TOA(S1) with a model that does not have this progress function. The class-wise detection results for both models are shown in Table 8. Under the same QA amount, there is a huge mAP difference of 5.3%. The progress function can help select balanced training samples among different classes to achieve performance boost in multiple object categories. In contrast, the model without the progress function tends to select redundant samples from major classes such as the “person” or the “car”. It does not find the most

critical examples to boost the overall detection performance, since samples of other object categories are not properly represented.

Third, we explain the hardness component in the progress function. By removing this component from the criticalness function, we show the result in Fig. 10(a), which has worse mAP performance under the same experimental setup using TOA(S3). It indicates that the hardness component plays an important role in highlighting different types of critical examples in different labeling stages.

Finally, we discuss the value of the representativeness component in the progress function. It is worthwhile to compare redundancy of samples in the VOC and the Caltech datasets. By examining the kNN graphs for both datasets, we find that the averaged Euclidian distance between two nearest samples is 249.3 and 1194.2 for the Caltech and the VOC07 datasets, respectively. In other words, samples in the Caltech dataset are closer than those in the VOC07 dataset. Based on this observation, we set $\delta = 0.2$ for the VOC dataset and $\delta = 1$ for the Caltech dataset, respectively, in adaptation to their different properties.

Effectiveness of NOP. We examine the quality of the NOP and the whole training samples. The quality of the NOP can be checked by calculating its precision of retrieving true negative samples. In the VOC07 dataset, the NOP algorithm can select an average of 1871 bounding boxes out of 1900 object proposals per images, meaning that a large percentage of boxes are still kept under the InvSet operation. For the whole NOP set, the negative sample precision is as high as 99.99914%. This is better than the precision of around 99.5% using alternative approaches as shown in Fig. 4. Recall that the NOP precision should be extremely high to avoid the network being confused by false negative.

The training samples in TOA include both QA-labeled samples and NOP samples. An example is shown in Fig. 11(a). In general, the visual quality of these training samples are high, where the NOP samples contain informative negative samples with different sizes. We also show the IoU histogram, which compares all NOP samples with the ground truth on the VOC07 dataset, in Fig. 11(b). Ideally, the IoU should fall in the range of TH_{HI} , TH_{LO} with full supervision. For the TOA method, the IOU values of the majority of negative samples are in the range.

Simulation Variation. We simulate human QA behavior in experiments. Humans can make inaccurate decision. Even if there is no intentional error, humans cannot determine objects based on a certain IoU threshold easily. For this reason, we add some random errors in the simulation. The original design is to ask humans to select objects with an IoU greater than 0.6. Here, we use a uniform random variable in

TABLE 8
Differences in detection results using models with/without the class-balancing progress function.

method	train set	aero	bike	bird	boat	bottle	bus	car	cat	chair	cow	table	dog	horse	mbike	person	plant	sheep	sofa	train	tv	mAP
TOA(S1)	07	42.9	61.5	40.9	19.0	24.6	55.3	59.2	55.0	21.7	56.0	33.8	47.4	60.1	58.6	43.0	21.9	45.4	41.9	52.6	44.7	44.3
TOA(S1) w/o balance	07	41.5	25.2	41.7	6.2	18.8	54.0	62.7	52.0	19.5	49.9	20.9	48.9	58.4	54.2	54.8	15.9	30.7	41.3	44.4	38.9	39.0

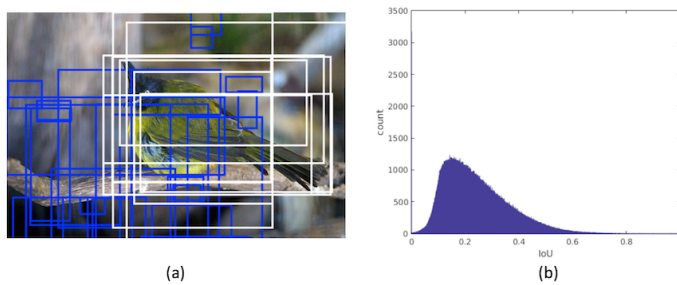


Fig. 11. Effectiveness of the NOP: (a) examples of training sample composition with 50 boxes, and (b) the IoU distribution of all negative samples as compared with the ground truth.

the range of $[0.6 + \psi, 0.6 - \psi]$ to simulate human thresholding. We set $\psi = 0.1$ and plot the results in Fig. 10(b). We see from the figure that the TOA method is robust against small labeling variations.

Labeling Time Model. Labeling time can vary according to the labeling tools. We apply the HQ profile time model that adopts numbers from several papers to provide an accurate estimation in the crowd sourcing setup. We also evaluate the time model using the MQ profile, which is in favor of the fully supervised learning. By following the experimental setup in Sec. 5.1, we show the results for the VOC07 dataset in Fig. 12(b). We still see clear performance gains of the TOA method over the full supervised one.

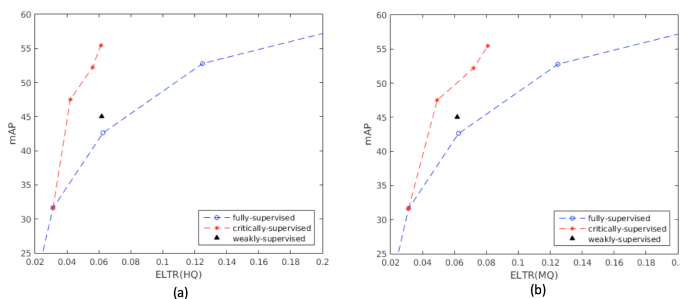


Fig. 12. Experimental results with different labeling time models: (a) the HQ profile and (b) the MQ profile.

6.6 Other Training Details

Being different from the traditional full supervision training, the TOA method has different types of training samples and follows an adaptive procedure in training the model. In this subsection, we briefly discuss how various training options affect the final results, and explain about our designed training details. Since the performance in Caltech dataset is superior and thus not sensitive to different training settings, we focus on the more complex VOC07 dataset.

Labeling Amount Selection. The selection of the labeling amount, including the number of initial fully labeled image

subset and the number of QA in each stage, is heuristic. It depends on the availability of annotation resources. Generally speaking, if a larger initial set is selected, detection scores and deep features are more reliable and better QA samples can be retrieved more efficiently. However, full-labeling is time consuming, leading to fast growth in labeling time. In contrast, if the initial set is too small, the poor S_0 detector will have bad performance in selecting CEM samples. In Fig. 13(a), we show the results with different initial sets, and then apply the same number of QA. In general, a smaller initial set is still favorable if the S_0 detector is not too poor. This is because QA-labeling consumes much less labeling time than full-labeling, and this choice will be more efficient in the early stage.

Bounding Box Regression (REG). Object detection involves multi-task training of probability scoring and bounding box regression simultaneously [17]. For bounding box regression, the ground truth bounding box locations are used as training targets. However, in the TOA method, we do not have ground truth bounding box locations. This limitation can be handled in several ways. The first one is to train the model without bounding box regression at all (with $REG=0$), which gives the worst performance in Fig. 13(b). An alternative solution is to accept the locations of these noisy bounding boxes as the ground truth with $REG=1$. We see from the figure that training the regressor with noisy bounding boxes still provide reasonable performance improvement. The result is better than that without any regression or using the weak regressor trained from the S_0 detector ($REG=2$). We also show the performance of the ideal case with an optimal regressor ($REG=3$), which is trained using the VOC2007 trainval set, in the figure for performance benchmarking. Our work emphasizes better on the classification performance. If accurate localization [9] is desired, a better regressor can be further added to the TOA method. In Sec. 6.3 and Sec. 6.4, we adopt $REG=1$, and for rest of the experiments we do not adopt bounding box regression for analysis purposes.

Pretrained Model Selection (PRETR). For each stage n , training samples are collected from both fully labeled and QA-labeled subsets. The training data set in stage n is always a superset of that in the previous stage. To retrain CNN model S_n , we have two choices: 1) using the ImageNet pretrained model ($PRETR=0$) as done in stage S_0 , or 2) applying the pretrained model from the previous stage and do fine-tuning ($PRETR=1$). For the latter, the learning rate can be reduced since it is built upon a better reference. The result is shown in Fig. 13(c). It shows that the directly retraining on ImageNet pretrained features results in better performances, which helps avoid bad feedback loop from previous training stages.

Weighing on Image Subsets (WTR). The TOA training set consists of both fully-labeled and QA-labeled subsets. The fully-labeled subset contain training samples of higher

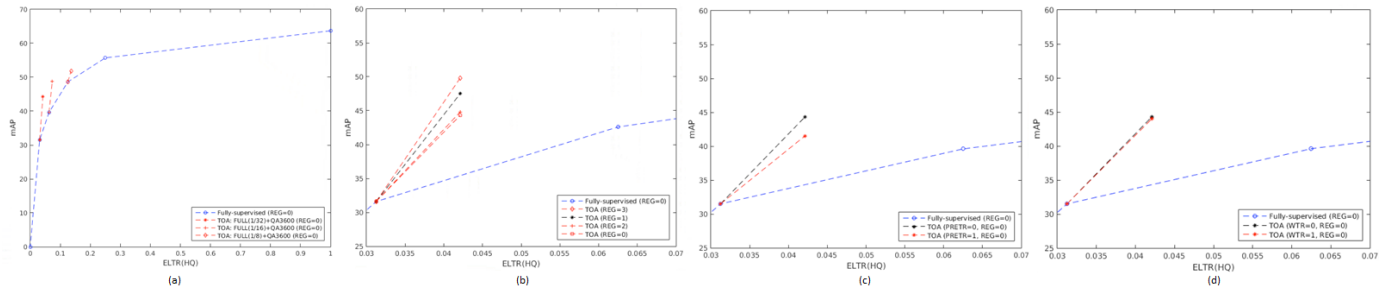


Fig. 13. Experimental results with different training parameters: (a) the size of the initial set, (b) bounding box regression (REG), (c) pretrained model selection (PRETR), (d) weighing on image subsets (WTR). Results are provided for a zoomed-in ELTR range except for (a).

quality than the QA-labeled subset. It could be advantageous to give the fully-labeled frames higher weights in the training process. This can be achieved by allowing the fully supervised frames to appear more times in each epoch (WTR=1). We show the result of weighing fully labeled images two times in Fig. 13(d). The weighting scheme does not provide better performance. It implies that the quality of training samples prepared by the TOA method is already good.

7 CONCLUSION

A critically supervised learning methodology for object detection was studied in this work with an objective to maintain good detection performance yet with significantly less labeling effort as compared with full supervision. Specifically, we proposed the TOA method that consists of several novel components. It used the CEM algorithm to select samples for QA and the NOP to extract negative samples without extra labeling. The effectiveness of the TOA method was demonstrated on the VOC dataset and the Caltech pedestrian dataset. Extensive experiments were conducted to provide insights into the TOA method.

REFERENCES

- [1] Z. Yan, J. Liang, W. Pan, J. Li, and C. Zhang, "Weakly-and semi-supervised object detection with expectation-maximization algorithm," *arXiv preprint arXiv:1702.08740*, 2017.
- [2] H. Bilen, M. Pedersoli, and T. Tuytelaars, "Weakly supervised object detection with posterior regularization," in *Proceedings BMVC 2014*, 2014, pp. 1–12.
- [3] R. Gokberk Cinbis, J. Verbeek, and C. Schmid, "Multi-fold mil training for weakly supervised object localization," in *Proceedings of the IEEE conference on computer vision and pattern recognition*, 2014, pp. 2409–2416.
- [4] H. Bilen, M. Pedersoli, and T. Tuytelaars, "Weakly supervised object detection with convex clustering," in *Proceedings of the IEEE Conference on Computer Vision and Pattern Recognition*, 2015, pp. 1081–1089.
- [5] O. Russakovsky, Y. Lin, K. Yu, and L. Fei-Fei, "Object-centric spatial pooling for image classification," *Computer Vision—ECCV 2012*, pp. 1–15, 2012.
- [6] H. O. Song, R. Girshick, S. Jegelka, J. Mairal, Z. Harchaoui, and T. Darrell, "On learning to localize objects with minimal supervision," *arXiv preprint arXiv:1403.1024*, 2014.
- [7] H. O. Song, Y. J. Lee, S. Jegelka, and T. Darrell, "Weakly-supervised discovery of visual pattern configurations," in *Advances in Neural Information Processing Systems*, 2014, pp. 1637–1645.
- [8] S. Li, X. Zhu, Q. Huang, H. Xu, and C.-C. J. Kuo, "Multiple instance curriculum learning for weakly supervised object detection." in *BMVC*, 2017.
- [9] D. P. Papadopoulos, J. R. Uijlings, F. Keller, and V. Ferrari, "We don't need no bounding-boxes: Training object class detectors using only human verification," in *Proceedings of the IEEE Conference on Computer Vision and Pattern Recognition*, 2016, pp. 854–863.
- [10] M. Everingham, S. M. A. Eslami, L. Van Gool, C. K. I. Williams, J. Winn, and A. Zisserman, "The pascal visual object classes challenge: A retrospective," *International Journal of Computer Vision*, vol. 111, no. 1, pp. 98–136, Jan. 2015.
- [11] P. Dollár, C. Wojek, B. Schiele, and P. Perona, "Pedestrian detection: An evaluation of the state of the art," *IEEE transactions on pattern analysis and machine intelligence*, vol. 34, no. 4, pp. 743–761, 2012.
- [12] P. F. Felzenszwalb, R. B. Girshick, and D. McAllester, "Cascade object detection with deformable part models," in *Computer vision and pattern recognition (CVPR), 2010 IEEE conference on*. IEEE, 2010, pp. 2241–2248.
- [13] P. Felzenszwalb, D. McAllester, and D. Ramanan, "A discriminatively trained, multiscale, deformable part model," in *Computer Vision and Pattern Recognition, 2008. CVPR 2008. IEEE Conference on*. IEEE, 2008, pp. 1–8.
- [14] R. Girshick, J. Donahue, T. Darrell, and J. Malik, "Rich feature hierarchies for accurate object detection and semantic segmentation," in *Proceedings of the IEEE conference on computer vision and pattern recognition*, 2014, pp. 580–587.
- [15] C. L. Zitnick and P. Dollár, "Edge boxes: Locating object proposals from edges," in *Computer Vision—ECCV 2014*. Springer, 2014, pp. 391–405.
- [16] J. R. Uijlings, K. E. van de Sande, T. Gevers, and A. W. Smeulders, "Selective search for object recognition," *International journal of computer vision*, vol. 104, no. 2, pp. 154–171, 2013.
- [17] R. Girshick, "Fast r-cnn," in *Proceedings of the IEEE International Conference on Computer Vision*, 2015, pp. 1440–1448.
- [18] K. He, X. Zhang, S. Ren, and J. Sun, "Spatial pyramid pooling in deep convolutional networks for visual recognition," in *European Conference on Computer Vision*. Springer, 2014, pp. 346–361.
- [19] S. Ren, K. He, R. Girshick, and J. Sun, "Faster r-cnn: Towards real-time object detection with region proposal networks," in *Advances in Neural Information Processing Systems*, 2015, pp. 91–99.
- [20] T. Kong, F. Sun, A. Yao, H. Liu, M. Lu, and Y. Chen, "Ron: Reverse connection with objectness prior networks for object detection," *arXiv preprint arXiv:1707.01691*, 2017.
- [21] J. Redmon, S. Divvala, R. Girshick, and A. Farhadi, "You only look once: Unified, real-time object detection," in *Proceedings of the IEEE Conference on Computer Vision and Pattern Recognition*, 2016, pp. 779–788.
- [22] J. Dai, Y. Li, K. He, and J. Sun, "R-fcn: Object detection via region-based fully convolutional networks," in *Advances in neural information processing systems*, 2016, pp. 379–387.
- [23] T. Kong, A. Yao, Y. Chen, and F. Sun, "Hypernet: Towards accurate region proposal generation and joint object detection," in *Proceedings of the IEEE Conference on Computer Vision and Pattern Recognition*, 2016, pp. 845–853.
- [24] W. Liu, D. Anguelov, D. Erhan, C. Szegedy, S. Reed, C.-Y. Fu, and A. C. Berg, "Ssd: Single shot multibox detector," in *European conference on computer vision*. Springer, 2016, pp. 21–37.
- [25] M. Shi, H. Caesar, and V. Ferrari, "Weakly supervised object localization using things and stuff transfer," *arXiv preprint arXiv:1703.08000*, 2017.
- [26] M. Shi and V. Ferrari, "Weakly supervised object localization using size estimates," in *European Conference on Computer Vision*. Springer, 2016, pp. 105–121.

- [27] T. Deselaers, B. Alexe, and V. Ferrari, "Weakly supervised localization and learning with generic knowledge," *International journal of computer vision*, vol. 100, no. 3, pp. 275–293, 2012.
- [28] A. J. Joshi, F. Porikli, and N. Papanikolopoulos, "Multi-class active learning for image classification," in *Computer Vision and Pattern Recognition, 2009. CVPR 2009. IEEE Conference on*. IEEE, 2009, pp. 2372–2379.
- [29] A. Kapoor, K. Grauman, R. Urtasun, and T. Darrell, "Active learning with gaussian processes for object categorization," in *Computer Vision, 2007. ICCV 2007. IEEE 11th International Conference on*. IEEE, 2007, pp. 1–8.
- [30] A. Kovashka, S. Vijayanarasimhan, and K. Grauman, "Actively selecting annotations among objects and attributes," in *Computer Vision (ICCV), 2011 IEEE International Conference on*. IEEE, 2011, pp. 1403–1410.
- [31] G.-J. Qi, X.-S. Hua, Y. Rui, J. Tang, and H.-J. Zhang, "Two-dimensional active learning for image classification," in *Computer Vision and Pattern Recognition, 2008. CVPR 2008. IEEE Conference on*. IEEE, 2008, pp. 1–8.
- [32] B. Siddiquie and A. Gupta, "Beyond active noun tagging: Modeling contextual interactions for multi-class active learning," in *Computer Vision and Pattern Recognition (CVPR), 2010 IEEE Conference on*. IEEE, 2010, pp. 2979–2986.
- [33] S. Vijayanarasimhan and K. Grauman, "Multi-level active prediction of useful image annotations for recognition," in *Advances in Neural Information Processing Systems*, 2009, pp. 1705–1712.
- [34] —, "What's it going to cost you?: Predicting effort vs. informativeness for multi-label image annotations," in *Computer Vision and Pattern Recognition, 2009. CVPR 2009. IEEE Conference on*. IEEE, 2009, pp. 2262–2269.
- [35] S. Branson, C. Wah, F. Schroff, B. Babenko, P. Welinder, P. Perona, and S. Belongie, "Visual recognition with humans in the loop," *Computer Vision—ECCV 2010*, pp. 438–451, 2010.
- [36] S. Vijayanarasimhan and K. Grauman, "Large-scale live active learning: Training object detectors with crawled data and crowds," *International Journal of Computer Vision*, vol. 108, no. 1-2, pp. 97–114, 2014.
- [37] X. Liang, S. Liu, Y. Wei, L. Liu, L. Lin, and S. Yan, "Towards computational baby learning: A weakly-supervised approach for object detection," in *Proceedings of the IEEE International Conference on Computer Vision*, 2015, pp. 999–1007.
- [38] Q. Zhang, R. Cao, Y. N. Wu, and S.-C. Zhu, "Mining object parts from cnns via active question-answering," *arXiv preprint arXiv:1704.03173*, 2017.
- [39] D. P. Papadopoulos, J. R. Uijlings, F. Keller, and V. Ferrari, "Training object class detectors with click supervision," *arXiv preprint arXiv:1704.06189*, 2017.
- [40] A. Shrivastava, A. Gupta, and R. Girshick, "Training region-based object detectors with online hard example mining," in *Proceedings of the IEEE Conference on Computer Vision and Pattern Recognition*, 2016, pp. 761–769.
- [41] C.-H. Wu, W. Gan, D. Lan, and C.-C. J. Kuo, "Boosted convolutional neural networks (bcnn) for pedestrian detection," in *2017 IEEE Winter Conference on Applications of Computer Vision*. IEEE, 2017, pp. 540–549.
- [42] H. Su, J. Deng, and L. Fei-Fei, "Crowdsourcing annotations for visual object detection," in *Workshops at the Twenty-Sixth AAAI Conference on Artificial Intelligence*, vol. 1, no. 2, 2012.
- [43] D. P. Papadopoulos, J. R. Uijlings, F. Keller, and V. Ferrari, "Extreme clicking for efficient object annotation," *arXiv preprint arXiv:1708.02750*, 2017.
- [44] J. Li, X. Liang, S. Shen, T. Xu, and S. Yan, "Scale-aware fast r-cnn for pedestrian detection," *arXiv preprint arXiv:1510.08160*, 2015.
- [45] K. Simonyan and A. Zisserman, "Very deep convolutional networks for large-scale image recognition," *arXiv preprint arXiv:1409.1556*, 2014.